

Tuning the Anodic and Cathodic Dissolution of Gold by Varying the Surface Roughness

Jeyabharathi Chinnaiah,^{*[a, c, g]} Olga Kasian,^[b] Amuthan Dekshinamoorthy,^[f, g] Saranyan Vijayaraghavan,^[f, g] Karl J. J. Mayrhofer,^[b, d, e] Serhiy Cherevko,^{*[b, d]} and Fritz Scholz^[c]

This work presents the reactivity and dissolution of an as-polished and electrochemically pre-treated polycrystalline Au electrode, which is used as a model system. The effect of the electrochemical pre-treatment in corrosive 0.37 M HCl solutions on the Au surface roughness and dissolution is investigated by varying the number of pre-treatment steps at 1.16 V against the reversible hydrogen electrode. It is shown that the first 10 s pre-treatment of the as-polished Au results in a higher surface roughness and thus higher electrochemically active surface area (ECSA) than that of the as-polished Au. With the subsequent pre-treatments, however, the ECSA is gradually decreasing reaching a steady value. The dissolution rate of the pre-treated Au electrodes upon potential cycling in 0.1 M H₂SO₄ is determined by in situ inductively coupled plasma mass spec-

trometry. A non-linear dependence of Au dissolution amount is found with respect to the number of pre-treatments. The overall total Au dissolution rate follows a similar trend as ECSA/roughness. However, an important difference in the dissolution behavior is identified with respect to dissolution processes during Au oxidation (anodic dissolution) and Au reduction (cathodic dissolution): the former is more sensitive to the surface roughness. Thus, the ratio between Au anodic and cathodic dissolution amounts decreases substantially with decrease in surface roughness. This finding is explained by the slow and fast dissolution kinetics for anodic and cathodic processes, respectively. Current work further advances our understanding of the complex Au dissolution mechanism.


1. Introduction

The reactivity of electrode surfaces depends on the presence of surface states such as surface defects^[1] The surface of mechanically polished polycrystalline gold electrodes has a microheterogeneous morphology with a disordered surface layer possessing features of a so called Beilby layer.^[2] This layer results from the variable energy input during the surface

preparation processes, explaining the different surface reactivity of as-prepared gold electrodes towards numerous electrode reactions. Moreover, preparation of reproducible gold surfaces by polishing is required to use them in electrochemical analysis, which is a troublesome task. The variability of the surface states of an as-polished gold electrode explains the typically observed differences in the range of measured data from electrochemical measurements.^[3] The absence of standard polishing protocols leads to additional problems in comparing the experimental results from different research groups. To circumvent these difficulties, electrochemists have developed electrochemical (or thermal) treatment procedures, which are extensively used in fundamental and applied studies^[4] One of the electrochemical approaches is to invoke repetitive gold oxidation and reduction cycles, which involve gold dissolution accompanied by oxidative stripping of impurities and (partial) re-deposition of dissolved gold species leading to the formation of a stable "clean" surface. Indeed, cyclic voltammograms of cleaned surfaces are well-known, which are used as a fingerprint of gold surface purity. The dissolution of such pretreated gold electrodes was studied in our previous works.^[5] Unfortunately, the reactivity of the stable surface-states to many surface sensitive reactions is moderate to poor. Many attempts have been made to understand and control the reactivity of gold, which is used as a model system.

To modify the surface reactivity, different approaches have been suggested. Most of them are based on chemical and electrochemical methods,^[7] although mechanical methods are also available.^[8] Nowicka et al.^[9] reported the deactivation of gold electrodes by selective knock-out of the active surface atoms using hydroxyl radicals. Surface deactivation has been

- [a] Dr. J. Chinnaiah
Electroplating & Metal Finishing Division, CSIR-Central Electrochemical Research Institute, Karaikudi – 630 003, Tamil Nadu, India
E-mail: cjeyabharathi@cecri.res.in
- [b] Dr. O. Kasian, Prof. K. J. J. Mayrhofer, Dr. S. Cherevko
Department of Interface Chemistry and Surface Engineering, Max-Planck-Institute of Iron Research, Max-Planck-Strasse 1, 40237 Düsseldorf, Germany
E-mail: s.cherevko@fz-juelich.de
- [c] Dr. J. Chinnaiah, Prof. F. Scholz
Institute of Biochemistry, University of Greifswald, Felix-Hausdorff-Strasse 4, 17487 Greifswald, Germany
- [d] Prof. K. J. J. Mayrhofer, Dr. S. Cherevko
Helmholtz-Institute Erlangen-Nürnberg for Renewable Energy (IEK-11), Forschungszentrum Jülich, Egerlandstrasse 3, 91058 Erlangen, Germany
- [e] Prof. K. J. J. Mayrhofer
Department of Chemical and Biological Engineering, Friedrich-Alexander-Universität Erlangen-Nürnberg, Egerlandstr. 3, 91058 Erlangen, Germany
- [f] Mr. A. Dekshinamoorthy, Dr. S. Vijayaraghavan
Corrosion and Materials Protection Division, CSIR-Central Electrochemical Research Institute, Karaikudi – 630 003, Tamil Nadu, India
- [g] Dr. J. Chinnaiah, Mr. A. Dekshinamoorthy, Dr. S. Vijayaraghavan
Academy of Scientific and Innovative Research (AcSIR), Ghaziabad – 201002, India

 © 2021 The Authors. ChemElectroChem published by Wiley-VCH GmbH. This is an open access article under the terms of the Creative Commons Attribution-NonCommercial-NoDerivs License, which permits use and distribution in any medium, provided the original work is properly cited, the use is non-commercial and no modifications or adaptations are made.

also achieved by repetitive Prussian blue formation and removal^[10] and by gold etching in cyanide solution in the presence of oxygen.^[11] Further, an electrochemical dissolution of gold to soluble gold species^[5a,b,12] can be used to control the surface states/morphology. By making use of metal dissolution and redeposition processes during an electrode reaction, surfaces can be activated/deactivated. For that, different types of electrochemical perturbation can be used, for example, repetitive square-wave perturbation,^[13] and potential cycling^[13b,14] or combination of both.^[15] These methods lead to a roughening or faceting/recrystallization of the surface. In this line, we reported that the mechanically polished polycrystalline gold can be electrochemically activated by potential cycling in 0.37 M HCl solution followed by potential cycling in 0.1 M H₂SO₄.^[16] In chloride solutions, the dissolution rate of gold is higher than in non-complexing electrolytes^[5c,17] Thus, at sufficiently positive potentials in complexing ions containing solutions, gold dissolution can be very appreciable. Compton et al.^[18] have used electrodisolution approach in chloride solutions to count and sort dispersed gold nanoparticles through nanoparticle impact experiments. Concerning the dissolution, there are few studies on as-polished gold electrodes.^[3,6]

In our previous work, we have shown that the anodic and cathodic dissolution depend on the Au coverage,^[19] that is, the anodic dissolution is coverage dependent, while cathodic dissolution is not. The current work aims to investigate the effect of roughness of gold electrodes on anodic and cathodic Au dissolution. The surface roughness was controlled by electrochemical oxidation of gold at constant potential in chloride solutions that depends on the number of dissolved gold layers. An anodic potential of 1.16 V vs RHE was applied for the dissolution of gold in HCl solutions, which is in the active dissolution potential region. This potential was chosen in such a way that the amount of gold dissolved upon 10 s treatments in HCl solutions would be reasonably small. The treated surfaces are tested by cyclic voltammetry in order to reveal whether the treatment in chloride solutions has an effect on surface roughness. After ensuring the changes in the electrochemically active surface area (ECSA) and the root-mean-squared roughness (RMS roughness) from AFM analysis, the system was used to study the effect of gold surface states on oxygen reduction reactions (ORR) and gold dissolution in sulfuric acid solutions. The dissolution of gold was analyzed in a potential resolved manner using a scanning flow cell (SFC) coupled with inductively coupled plasma mass spectrometer ICP-MS (in-situ ICP-MS).^[5a,b] This setup allowed us to resolve and quantify both the anodic and cathodic gold dissolution. The obtained results show that anodic dissolution is scaled with ECSA and roughness, while the cathodic dissolution is less-affected. For a stabilized gold surface with the lower ECSA and physical roughness, the ratio of the anodic to the cathodic dissolution has become constant.

Experimental Section

Sulfuric acid (either 98%, Emsure® for analysis or Suprapur 96%) and hydrochloric acid (35%, Emsure® for analysis), and potassium nitrate (Merck, Emsure® for analysis) were obtained from Merck. All the solutions were prepared using Millipore water (PureLab Plus system, Elga, 18 MΩ cm, TOC < 3 ppb) and the temperature was maintained at 25 °C.

Polycrystalline gold disk electrodes with a diameter of 2 mm and 8 mm were used as working electrodes. The electrodes were mechanically polished on a polishing pad (from Buhler) using slurries made from 1 μm and 0.3 μm Al₂O₃ powders, cleaned well by sonication in Millipore water for 2 minutes and finally rinsed with Millipore water. Such cleaned electrode is denoted as “as-polished electrode”. A three-electrode cell configuration connected to an Autolab potentiostat (Metrohm) was used for quiescent electrochemical experiments. A glassy carbon (GC) rod (from Metrohm) was used as the counter electrode, and an Ag/AgCl (3 M KCl) electrode (from Metrohm) as reference ($E = 0.210$ V vs RHE). The reference electrode was separated from the electrolyte by KNO₃-agar salt bridges (polyethylene tubing filled with the salt-gel). However, all the potentials were referred to the reversible hydrogen electrode (RHE) scale. For the oxidative dissolution of gold in chloride medium at 1.16 V for 10 s (six independent treatments on the same electrode), deaerated 0.37 M HCl solution was used. The surface roughness of the treated gold electrodes was analysed using AFM. The AFM analysis was performed using a scanning probe microscope (Agilent technologies, USA. 5500 series). The software used for imaging was pico view 1.14.1. The obtained raw images were processed using WSxM 5.0. Further, the treated gold electrodes were used to study the ORR, which was used as a probe reaction in O₂ saturated 0.1 M H₂SO₄ solutions. Unless otherwise mentioned, the electrolytes were deaerated by purging the electrolytes with nitrogen for 20 minutes before the measurements and a nitrogen blanket was maintained throughout the measurements.

The electrochemical dissolution measurements on treated gold electrodes were performed using an electrochemical scanning flow cell (SFC) coupled with an inductively coupled plasma mass spectrometer (ICP-MS, NexION 300X, Perkin Elmer).^[5a,b] A Gamry Reference 600, USA potentiostat was used for the electrochemical measurements with this setup. All presented results were normalized to the geometric area of the working electrode (ca. 0.01 cm²). A saturated Ag/AgCl electrode (Metrohm, Germany) and a graphite rod, placed in the inlet channel of the SFC, were utilized as the counter and reference electrodes, respectively. All reported potentials were referenced to the RHE potential, that was measured every day using a polycrystalline Pt foil (99.99%, MaTeck, Germany) in hydrogen saturated 0.1 M H₂SO₄. After saturation with Ar, this solution was also used in electrochemical measurements. Prior to the introduction into the ICP-MS, the electrolyte was mixed with an internal standard in a Y-connector (mixing ratio 1:1) after the electrochemical cell. As internal standard for the determination of dissolved Au, a solution containing 10 μg L⁻¹ of Re was used. The ICP-MS was calibrated every day of the experiment prior to the electrochemical measurements. Electrochemical surface area (ECSA) was calculated by normalizing the measured gold oxide reduction charge with 400 μC cm⁻².^[20]

2. Results and Discussion

To control the surface roughness, as-polished gold electrode was treated by potentiostating it at 1.16 V vs RHE for 10 s in 0.37 M HCl solutions. A complex gold dissolution mechanism

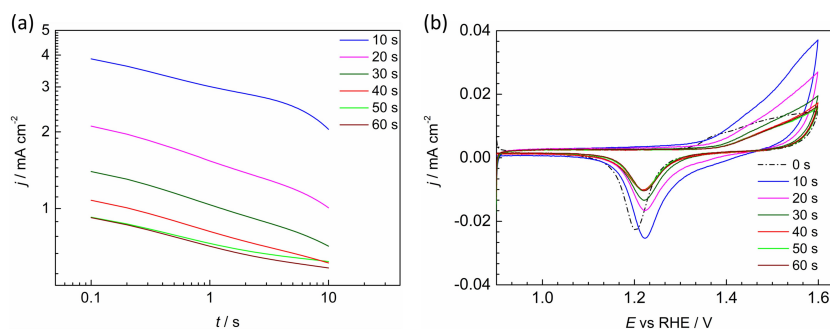
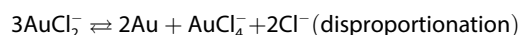
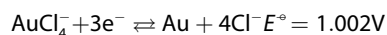
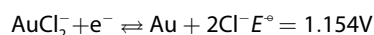


Figure 1. (a) j - t transient curves (as a log-log plot) of gold dissolution at 1.16 V vs RHE in 0.37 M HCl solution; (b) Cyclic voltammograms of gold electrode in 0.1 M H₂SO₄ recorded in parallel to dissolution measurements using SFC-ICP-MS after each 10 s of treatment in 0.37 M HCl solution. Scan rate: 2 mV s⁻¹.

has been proposed in chloride solutions that involves many elementary steps, viz., adsorption of chloride on gold by partial charge transfer and further electrooxidation to various adsorbed chlorinated gold species and their desorption to chlorinated gold solution species.^[21] The following equations (at standard conditions) describe the processes at the interface after the initial adsorption of chloride on gold:



Thus, thermodynamically, the employed gold dissolution potential (1.16 V vs RHE in 0.37 M HCl solutions) favours the formation of soluble gold chloride species.^[5c,22] The protocol was successively repeated several times until the establishment of a stable j - t transient response, pointing to the formation of a surface with a stable ECSA (Figure 1a). The amount of gold dissolved during the successive 10 s treatments can be estimated by integrating the j - t transient curves and applying Faraday's law. The estimated amounts of gold from the j - t transient curves presented in Figure 1a are given in Table 1. Here, AuCl₄⁻ was considered as the main product in aq. 0.37 M HCl solution,^[5c,18] although the formation of AuCl₂⁻ species can not be excluded. The latter could undergo a disproportionation reaction to Au and AuCl₄⁻. For our calculation, 100% current efficiency of dissolution was assumed to be operative. However,

a fraction of the anodic current originates from the oxidation of impurities, which might have entered onto the gold surface during mechanical polishing. Thus, the real current efficiency may be slightly lower, especially for the first treatment.

During the first 10 s anodic step in HCl solutions, ca. 16 μg cm⁻² of gold was dissolved. Further successive treatments resulted in a gradual decline of the amount of dissolved gold. After the fourth 10 s treatment, the dissolution reached a steady value of ca. 4 μg cm⁻² (see Table 1) per treatment. The latter value corresponds to the dissolution rate of ca. 1 monolayer (ML) of gold per second (1 ML is ca. 400 ng cm⁻²,^[5a,5b] roughness neglected), assuming a constant dissolution rate (a rough estimation as dissolution decreases with time as shown in Figure 1a). After the total 60 s treatment, the amount of gold dissolved was ca. 42 ML equivalents, which implies that unlike dissolution by OH radical treatment^[9] dissolution process is not selective to asperities. But, the dissolution trend from 10 s to 60 s treatment time is similar to the one observed by Nowicka et al.,^[9a] although the dissolution has ceased to take place after certain number of treatments with hydroxyl radicals. This was due to selective removal of asperities leading to decreasing dissolution rates. However, in our anodic dissolution case, the chemistry of gold dissolution might differ from that in Nowicka's experiments. The most important difference is that these anodic treatments were performed in an electrolyte containing strong complexing ligand, viz., chloride ions, where dissolution might take place almost at all the surface sites leading to the formation of soluble gold chloride species. But, the Nowicka's experiment involved the formation of a gold oxide monolayer followed by a partial dissolution. Providing that if they had chloride in the solutions, the dissolution might not be selective as the oxides can be chemically removed by chloride ions. Thus, in non-complexing solutions, the differences in the energies of surface atoms must be much more important.

Since the calculated amount of dissolved gold decreased significantly after the initial 10 s anodic treatments and became steady with the subsequent ones, the surface area might be different after each treatment. To test this, we run a cyclic voltammogram immediately after the dissolution experiment in 0.1 M sulfuric acid. The CVs measured after each anodic treatment are presented in Figure 1b, which shows a typical gold oxide formation and oxide reduction response. In the

Table 1. Amount of gold dissolved at 1.16 V vs RHE during each 10 s treatment in 0.37 M HCl solution calculated using Faraday's law from data presented in Figure 1a. ECSA was calculated by integrating the oxide reduction peak on the cathodic branch of the CVs in Figure 1b.

Time at 1.16 V [s]	Au dissolved in HCl _{aq} [μg cm ⁻²]	ECSA [cm ²]
0	–	0.0225
10	16.24	0.0343
20	7.80	0.0231
30	5.41	0.0172
40	4.33	0.0138
50	4.05	0.0139
60	4.23	0.0134

cyclic voltammograms, a small positive shift in the reduction peak potential was observed after the treatments, indicating the formation of more easily reducible oxides. The first CV was used to calculate the ECSA by normalizing the measured gold oxide reduction charge with $400 \mu\text{Ccm}^{-2}$, because the treatment in chloride containing electrolyte might lead to a stable surface as a result of faster diffusion of surface atoms to the suitable lattice sites on the surface^[23] We avoided multiple CVs to ensure that the surface condition of the gold was not changed due to recrystallization.^[24] The gold dissolution trend deduced from the $j-t$ transient curve corroborates well with the ECSA calculated from the CVs with respect to the treatment time (see Table 1).

To better understand the observed variation in ECSA, we performed AFM topographic imaging on the as-polished surface as well as on the surface after each successive anodic treatments. The recorded AFM images are presented in Figure 2 (a–g). The root-mean-squared roughness value was calculated and was plotted with respect to treatment times (Figure 2h). The as-polished surface exhibited a surface topography of mechan-

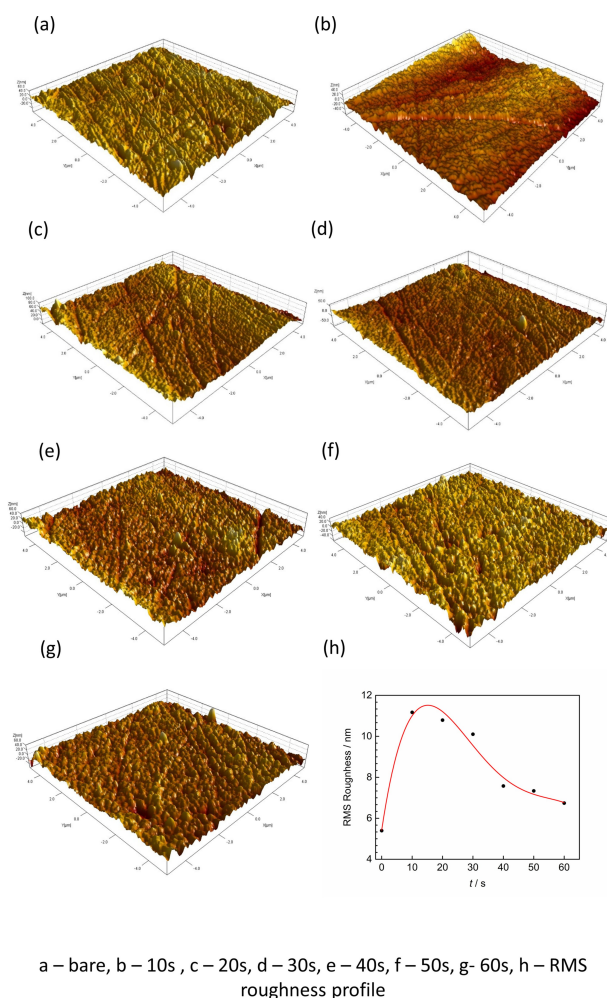


Figure 2. AFM-topographic images of as-polished (a) and treated electrodes for 10 s (b), 20 s (c), 30 s (d), 40 s (e), 50 s (f) and 60 s (g). The plot (h) shows the root-mean squared roughness (nm) profile with respect to electrochemical treatment time.

ically polished surface with the typical scratches and had a surface roughness of 5.4 nm. After the first 10 s anodic treatment, the topography changed to a rougher one and the roughness was increased to 11.2 nm. With the subsequent 10 s treatments up to 40 s, a significant decline in the roughness value was noticed, i.e., from 11.2 nm after 10 s to 7.6 nm after 40 s treatment times. Then, the roughness did not vary much further and reached a roughness value of 6.7 nm after 60 s treatment. From the CV and the AFM, the trend in ECSA is in line with the variation in the physical roughness. However, the smoothing effect is not as significant as observed in the work of Nowicka et al.^[9a] As discussed above, the different chemistry of gold dissolution in complexing medium could be the possible reason for not observing the smoothed surface. Thus, in a complexing (reactive) chloride solutions, anodic oxidation of polycrystalline gold lead, after repetitive treatments, to a rather constant and still rough surface.

The changes in the roughness/ECSA might influence the reactivity^[4,5] of the treated surface towards surface sensitive reactions like oxygen reduction reaction (ORR) and we tested the treated surfaces for the ORR, which is an innersphere electrode reaction in acidic solutions.^[9b,16] Figure 3 shows the half-peak potential ($E_{p/2}$) of the ORR vs treatment time. The ORR activity followed the same trend as the ECSA with respect to the number of treatments, i.e., the $E_{p/2}$ shifted to positive potentials (higher catalytic activity) with an increase in ECSA after the initial 10 s treatment and then it shifted to negative values until 40 s and then became constant within the subsequent treatments. The ORR experiment further strengthened the fact that surface condition was tuned upon anodic treatment in HCl solutions potentiostatically that was even reflected in the reactivity profile with respect to number of treatments. Since gold adsorbs oxygenated species weakly, it requires a highly defective surface structure to activate the ORR processes. So, after the initial 10 s treatment in HCl solutions, the ECAS was high signifying the availability of a larger number of lowcoordinated surface sites, which may be directly correlated to the higher $E_{p/2}$. With the subsequent treatments, the $E_{p/2}$

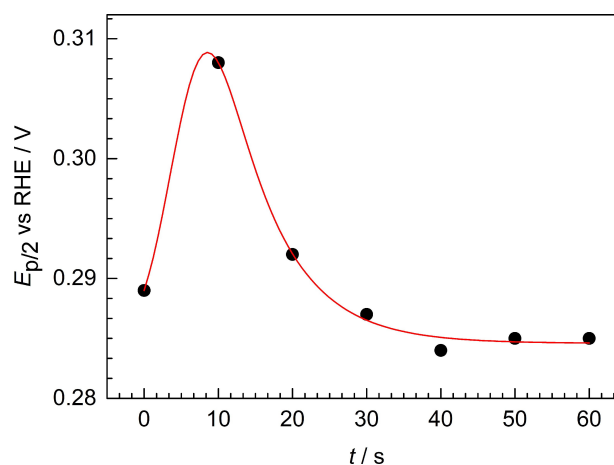


Figure 3. Plot of the ORR half-peak potential measured on gold electrode versus anodic treatment time of the gold in 0.37 M HCl solution at 1.16 V.

Time at 1.16 V [s]	Anodically dissolved gold [ng cm ⁻²]	Cathodically dissolved gold [ng cm ⁻²]	Total dissolved gold [ng cm ⁻²]
0	28.41	8.07	36.48
10	76.45	20	96.45
20	46.52	15.80	62.32
30	29.70	14.60	44.30
40	19.10	10.60	29.70
50	22.27	12.34	34.61
60	22.34	12.75	35.09

2 scaled with the decrease in the ECAS, indicating the formation of relatively more stable surface having less defective sites.

After validating the effect of successive anodic dissolution steps in 0.37 M HCl solutions at 1.16 V vs RHE on the surface roughness, we performed dissolution experiment on the treated surfaces in 0.1 M H₂SO₄ solutions under cyclic voltammetry condition using the SFC-ICP-MS setup. To proceed with, the electrode was first stepped to 1.16 V for 10 s in 0.37 M HCl solutions and then the treated electrode was cleaned well with ultrapure water and was dried under a stream of Ar. The surface state of gold was tested by recording a CV in a typical gold oxidation/reduction region in 0.1 M H₂SO₄ using the SFC-ICP-MS setup. Parallely, dissolution profiles were also recorded in a time synchronized manner. Figure 4(a–d) shows the representative dissolution profiles of the as-polished and 10 s, 20 s, 40 s, and 60 s treated gold electrodes during a CV run at 0.01 V/s in 0.1 M H₂SO₄. The dissolution profiles have two peaks and the first is related to anodic dissolution followed by a second one, which is related to cathodic dissolution. Table 2 presents the amount of gold dissolved, which was obtained by integrating

the corresponding deconvoluted peaks of dissolution profiles (dissolution rate, ng cm⁻² s⁻¹). The total dissolved amount of gold (both during anodic and cathodic dissolution) after a 10 s treatment is ca. 2.5 times (95.5 ng cm⁻²) which is higher than that of the as-polished electrode itself (36.5 ng cm⁻²) (see Table 2). This is due to increase in surface roughness after the initial treatment of as-polished polycrystalline gold in 0.37 M HCl solutions for 10 s and/or surface cleaning, which in turn accelerated the dissolution. Upon subsequent treatment (from 10 s to 60 s), the total dissolved amount of gold dropped from 95.5 ng cm⁻² to steady values of ca. 35 ng cm⁻² (Table 2 and Figure 5a). Interestingly, the resolved anodic profile exhibited variations with respect to the changes in ECSA/roughness of the gold electrode. While there is a substantial decrease in the rate and amount of anodic dissolution, the cathodic dissolution is less-affected by the roughness (Table 2 and Figure 5a). This is clearly reflected in the ratio of the anodically dissolved gold to cathodically dissolved gold (obtained by deconvolution of corresponding peaks in dissolution profiles) that declined more by a factor of two from ca. 3.8 to 1.75 for 10 s and 60 s treatments of the gold surfaces, respectively (Figure 5b). Notably, the total dissolved amount was 35 ng cm⁻² (table 2) and the rate of dissolution is significant after 60 s treatment.

The observed difference in the anodic and cathodic dissolution sensitivity towards the surface roughness can be related to both dissolution kinetics and mass transfer of dissolved species. While substantial knowledge on gold dissolution has been acquired over the last several years, in particular with the help of SFC-ICP-MS,^[5–6] the mechanism of anodic and cathodic gold dissolution in electrolytes free of complexing ions is still lacking. We proposed earlier several tentative mechanisms to explain both anodic and cathodic dissolution.^[5b] Thus, it was suggested that at lower positive potentials (before the onset of oxygen evolution reaction

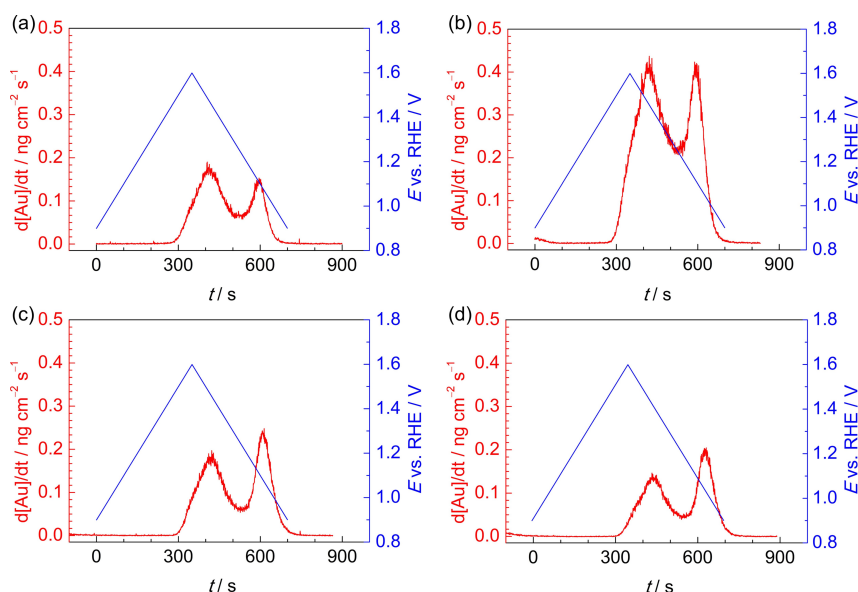


Figure 4. Dissolution profiles recorded (a) before and after (b) 10 s, (c) 30 s and (d) 60 s treatment in 0.37 M HCl solutions. Red lines: dissolution rate; blue lines: applied potential waveform.

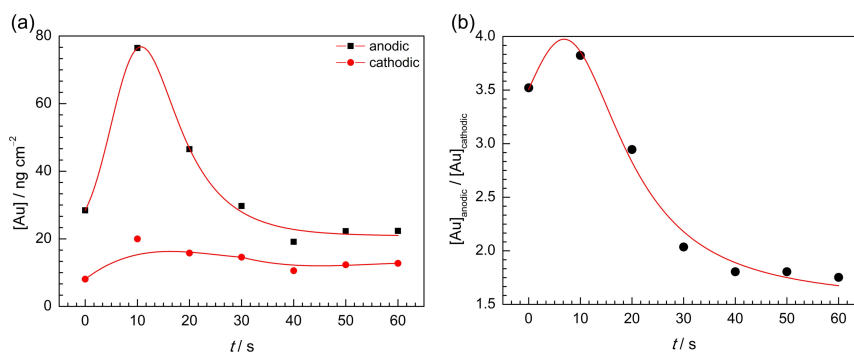


Figure 5. (a) Amount of anodically and cathodically dissolved gold versus treatment time obtained by deconvolution of the corresponding peaks in dissolution profiles represented in Fig. 4; (b) the ratio between anodically and cathodically dissolved gold depending on the treatment time.

(OER)), a transient anodic gold dissolution was caused by the surface disruption following an irreversible place exchange-like oxidation processes. Consequently, the reverse reduction process was assumed as a trigger for cathodic dissolution.^[5a,b] In a very recent work, an attempt was made to correlate experimental data on dissolution kinetics of noble metals with available thermodynamic data^[25] The main outcome of that work was that the same macroscopic process of Au/Au³⁺ transition is responsible for both anodic and cathodic dissolution. As the surface state is very different (metal to oxide and oxide to metal transition for anodic and cathodic dissolution, respectively), gold dissolution during forward and reverse scan is not equal. Typically, anodic dissolution dominates. In some cases, however, as for the platinum covered gold, where coverage of the gold atoms exposed to electrolyte is tuned by the amount of platinum, the cathodic dissolution was the main dissolution process.^[19] In fact, the anodic dissolution of both platinum and gold was coverage dependant, whereas the cathodic dissolution was not. As platinum was used in that work, electronic effects influencing dissolution cannot be excluded. The experimental results in the current work, where pure gold electrodes were used, are in line with our previous finding. It seems that the anodic dissolution is a slow process, which might probably be related to the sluggish kinetics of the metallic gold lattice rupture during the place exchange. Hence, at any given potential, the concentration of the dissolved species in the vicinity of the electrode surfaces is lower than the equilibrium one according to the Nernst equation. On the other hand, the cathodic dissolution is a fast process that can be again related to the faster kinetics of oxide reduction. It also takes place at relatively low anodic potentials, which ensures that a local equilibrium is formed (dissolution extent is controlled by mass transfer from the electrode into the bulk of electrolyte). Obviously, in this case, the dissolution amount is coverage (ECSA or roughness) independent. As an indirect confirmation for this statement, one can consider the shape of typical dissolution profiles (Figure 4), on which the cathodic peaks are sharper.

3. Conclusions

Careful control over the surface roughness of gold electrode was achieved by successive 10 s anodic treatment at 1.16 V in 0.37 M HCl solutions. The ECSA was estimated from the cyclic voltammetric curve of the treated surface in 0.1 M H₂SO₄, which was found to change non-linearly and the ECSA trend agreed well with the physical roughness obtained from AFM measurements. The reported experiments show that in a complexing (reactive) solution, here a chloride solution, anodic oxidation of polycrystalline gold leads, after repetitive treatments, to a rather constant and still rough surface. The ORR reactivity of the treated surfaces is also in agreement with the observed trend in roughness/ECSA measured on those surfaces. Further, the treated gold was used as a model in the investigation of the surface roughness dependent gold dissolution. We established that the anodic dissolution scales with surface area/roughness, while the cathodic dissolution was less-affected. Thus, the ratio of the anodic to the cathodic dissolution dropped more than by a factor of two from 3.85 to 1.72 between the first and the sixth treatment. This behaviour was explained by the slow anodic and fast cathodic dissolution kinetics. It is suggested that the latter process is controlled by mass transfer of the dissolved species from the vicinity of the electrode.

Conflict of Interest

The authors declare no conflict of interest.

Keywords: gold dissolution · corrosion · dissolution mechanism · in situ-ICP-MS · surface state

- [1] a) G. Ertl, *Angew. Chem. Int. Ed.* **2008**, *47*, 3524–3535; *Angew. Chem.* **2008**, *120*, 3578–3590; b) L. D. Burke, P. F. Nugent, *Gold Bull.* **1997**, *30*, 43–53.
 [2] A. D. Vlasov, J. S. Rez, M. L. Fil'chenkov, *Cryst. Res. Technol.* **1988**, *23*, 1093–1100.
 [3] S. Cherevko, *J. Electroanal. Chem.* **2017**, *787*, 11–13.
 [4] a) P. Rodriguez, M. T. M. Koper, *Phys. Chem. Chem. Phys.* **2014**, *16*, 13583–13594; b) J. C. Hoogvliet, M. Dijkstra, B. Kamp, W. P. van Benne-

- kom, *Anal. Chem.* **2000**, *72*, 2016–2021; c) L.-H. Guo, J. S. Facci, G. McLendon, R. Mosher, *Langmuir* **1994**, *10*, 4588–4593.
- [5] a) S. Cherevko, A. A. Topalov, I. Katsounaros, K. J. J. Mayrhofer, *Electrochem. Commun.* **2013**, *28*, 44–46; b) S. Cherevko, A. A. Topalov, A. R. Zeradjanin, I. Katsounaros, K. J. J. Mayrhofer, *RSC Adv.* **2013**, *3*, 16516–16527; c) O. Kasian, N. Kulyk, A. Mingers, A. R. Zeradjanin, K. J. J. Mayrhofer, S. Cherevko, *Electrochim. Acta* **2016**, *222*, 1056–1063.
- [6] S. Cherevko, A. R. Zeradjanin, A. A. Topalov, N. Kulyk, I. Katsounaros, K. J. J. Mayrhofer, *ChemCatChem* **2014**, *6*, 2219–2223.
- [7] C. Jeyabharathi, U. Hasse, P. Ahrens, F. Scholz, *J. Solid State Electrochem.* **2014**, *18*, 3299–3306.
- [8] V. C. Noninski, *J. Electroanal. Chem. Interfacial Electrochem.* **1989**, *267*, 287–290.
- [9] a) A. M. Nowicka, U. Hasse, M. Hermes, F. Scholz, *Angew. Chem. Int. Ed.* **2010**, *49*, 1061–1063; *Angew. Chem.* **2010**, *122*, 1079–1081; b) A. M. Nowicka, U. Hasse, G. Sievers, M. Donten, Z. Stojek, S. Fletcher, F. Scholz, *Angew. Chem. Int. Ed.* **2010**, *49*, 3006–3009; *Angew. Chem.* **2010**, *122*, 3070–3073.
- [10] P. Esakki Karthik, C. Jeyabharathi, S. Senthil Kumar, K. L. N. Phani, *J. Solid State Electrochem.* **2013**, *17*, 3055–3061.
- [11] C. Jeyabharathi, U. Hasse, P. Ahrens, F. Scholz, *J. Solid State Electrochem.* **2014**, *18*, 3299–3306.
- [12] a) S. Vesztergom, M. Ujvári, G. G. Láng, *Electrochem. Commun.* **2011**, *13*, 378–381; b) S. Vesztergom, M. Ujvári, G. G. Láng, *Electrochim. Acta* **2013**, *110*, 49–55.
- [13] a) C. L. Perdriel, A. J. Arvia, M. Ipohorski, *J. Electroanal. Chem.* **1986**, *215*, 317–329; b) A. C. Chialvo, W. E. Triaca, A. J. Arvia, *J. Electroanal. Chem. and Interf. Electrochem.* **1984**, *171*, 303–316; c) M. E. Vela, S. L. Marchiano, R. C. Salvarezza, A. J. Arvia, *J. Electroanal. Chem.* **1995**, *388*, 133–141.
- [14] a) T. Izumi, I. Watanabe, Y. Yokoyama, *J. Electroanal. Chem. Interfacial Electrochem.* **1991**, *303*, 151–160; b) C. Köntje, D. M. Kolb, G. Jerkiewicz, *Langmuir* **2013**, *29*, 10272–10278.
- [15] M. E. Martins, J. J. Podesta, A. J. Arvia, *Electrochim. Acta* **1987**, *32*, 1013–1017.
- [16] C. Jeyabharathi, P. Ahrens, U. Hasse, F. Scholz, *J. Solid State Electrochem.* **2016**, *20*, 3025–3031.
- [17] M. Tian, W. G. Pell, B. E. Conway, *Corros. Sci.* **2008**, *50*, 2682–2690.
- [18] Y.-G. Zhou, N. V. Rees, J. Pillay, R. Tshikhudo, S. Vilakazi, R. G. Compton, *Chem. Commun.* **2012**, *48*, 224–226.
- [19] S. Cherevko, G. P. Keeley, N. Kulyk, K. J. J. Mayrhofer, *J. Electrochem. Soc.* **2016**, *163*, H228–H233.
- [20] S. Trasatti, O. A. Petrii, *J. Electroanal. Chem.* **1992**, *327*, 353–376.
- [21] a) A. Kolics, A. E. Thomas, A. Wieckowski, *J. Chem. Soc. Faraday Trans.* **1996**, *92*, 3727–3736; b) D. S. Ramírez-Rico, E. R. Larios-Durán, *J. Electrochem. Soc.* **2017**, *164*, H994–H1002.
- [22] M. Orlik, *Self-Organization in Electrochemical Systems I: General Principles of Self-organization. Temporal Instabilities*, Springer Berlin Heidelberg, **2012**.
- [23] M. Mesgar, P. Kaghazchi, T. Jacob, E. Pichardo-Pedrero, M. Giesen, H. Ibach, N. B. Luque, W. Schmickler, *ChemPhysChem* **2013**, *14*, 233–236.
- [24] C. Jeyabharathi, M. Zander, F. Scholz, *J. Electroanal. Chem.* **2018**, *819*, 159–162.
- [25] S. Cherevko, in *Reference Module in Chemistry, Molecular Sciences and Chemical Engineering*, Elsevier, **2017**.

Manuscript received: March 19, 2021

Revised manuscript received: April 2, 2021

Accepted manuscript online: April 13, 2021